Int. J. Electrochem. Sci., 13 **(2018)** 2430 – 2440, doi: 10.20964/2018.03.71

International Journal of
ELECTROCHEMICAL
SCIENCE
www.electrochemsci.org

Short Communication

The Interactions between High Temperature Water and Fe_3O_4(111) by First-Principles Molecular Dynamics Simulation

Haitao Wang[1, *], *Xianfeng Sun*[1,2], *En-Hou Han*[1]

[1] CAS Key Laboratory of Nuclear Materials and Safety Assessment, Institute of Metal Research, Chinese Academy of Sciences, Shenyang 110016, China
[2] School of Materials Science and Engineering, University of Science and Technology of China, Hefei 230026, China
[*]E-mail: htwang@imr.ac.cn

Received: 11 december 2017 / *Accepted:* 16 January 2018 / *Published:* 5 February 2018

The interactions between high temperature water and oxide film Fe_3O_4(111) are investigated using a Born-Oppenheimer molecular dynamics simulation within the framework of density functional theory. A periodic twelve-layer slab covered with 21 water molecules is employed to simulate the interfacial reaction behavior. It can be observed in the simulation that the spontaneous dissociation processes of H_2O molecules occur on the Fe_3O_4(111) surfaces and the partial density of states demonstrates the hybridization bonding between 2p orbital of O atom and 3d orbital of Fe atom. There is an obvious charge transfer between the oxide film/electrolyte interface, whereas the charge transfer of the middle layers of substrate and solution is not significant.

Keywords: Magnetite; High temperature water; First principles molecular dynamics; Interfacial reaction

1. INTRODUCTION

The austenitic stainless steels have been widely used as structure materials in nuclear power plants because of theirs excellent mechanical properties and corrosion resistance [1-2]. The corrosion of stainless steel in high temperature water of nuclear power plants is an electrochemical process, and the oxide films formed by corrosion can prevent the further interactions between metal substrate and electrolyte [3-5]. The nucleation and propagation of localized corrosion, and stress corrosion cracking in particular, are related to the properties of the oxide film formed on the surface. A number of studies [6-10] have been performed to clarify the characteristics of these oxide films, and confirmed that the structure and composition of oxide films depend on the chemical composition of the alloy and the water chemistry conditions. On the basis of quantitative chemical descale, X-ray diffraction and

electron microprobe analyses, it is generally accepted that these oxide films have a double-layer structure. The outer oxide mainly consists of magnetite Fe_3O_4 crystallites, while the underlying inner oxide is composed of chromium-rich spinel. Stellwag [11-13] suggested that the inner layer is formed by solid-state growth processes, while the outer layer by the precipitation of metal ions released from the corroding surface or from elsewhere to the fluid.

Because the outer oxide film Fe_3O_4 is directly in contact with the electrolyte, its interface reaction behavior is a key step towards understanding the nature of corrosion. However, the experimental techniques are very difficult to obtain detailed information due to the complexity of the system and its various nonlinear interactions, so that its microscopic mechanism is still lacking to some extent. With large advances in the computational technology, the usage of numerical modeling methods which are computationally intensive such as first principles molecular dynamics simulation has become more feasible to address the metallic oxide-electrolyte interface and allow direct observation of some atomic scale phenomena. In the field of first principles molecular dynamics, the Born-Oppenheimer molecular dynamics have a higher computational accuracy and reliability than other methods [14-16]. Jul et al. [17] studied the stability of water structures on the perfect MgO(100) surface at room temperature using Born-Oppenheimer molecular dynamics simulation. Costa et al. [18] performed the investigation of water interaction on the Cr_2O_3(0001) surfaces at room temperature based on Born-Oppenheimer approach. However, to our knowledge, there have been no previous reports on the interfacial reaction behavior of oxide film Fe_3O_4 in high temperature water based on this approach. In the present work, we use a Born-Oppenheimer molecular dynamics simulation to investigate the interactions between high temperature water and oxide film Fe_3O_4(111), and provide fundamental information for understanding theirs interface characteristics at an electronic/atomic scale.

2. COMPUTATIONAL METHODS

The work was performed within the first-principles density functional theory (DFT) by using the projector-augmented plane wave(PAW) method of a plane wave basis implemented in the Vienna ab initio simulation package (VASP) [19, 20]. The exchange and correlation energies were described using the spin-polarized generalized gradient approximation and Perdew–Burke–Ernzerhof functional (GGA-PBE) [21]. The electronic wave function was expanded in a plane-wave basis set up to an energy cutoff of 400 eV. The Fe-$3d^6 4s^2$, O-$2s^2 2p^4$ and H-$1s^1$ electrons were treated as valence electrons. The Monkhorst-Pack scheme was used for the k-point sampling, and the integration over the Brillouin zone was carried out with the Γ point of the supercell. The convergence criteria of forces and energies were 0.05 eV/Å and 10^{-4} eV respectively. A Methfessel−Paxton electronic energy smearing of 0.2 eV was used to improve the convergences. The conjugate-gradient method was used for the geometry optimizations. The molecular dynamics calculation was performed within the microcanonical ensemble using a time step of 1 fs, for up to 3 ps. A Verlet algorithm was used to integrate the equations of motion, and a target temperature of 593.15 K based on the actual operating condition in the primary loop of pressurized water reactor was controlled by the velocity scaling method.

The system was represented by a Fe_3O_4 supercell having dimensions 11.5056 Å×11.5056 Å×8.3795 Å and α=90º, β=90º, γ=120º, which contained a twelve-layer slab, with 48 Fe atoms and 64 O atoms in total. The exposed face of the slab was the (111) surface because it was known to exhibit one of the lowest energy for Fe_3O_4 structure. A vacuum layer of 10 Å along the z-direction perpendicular to the surface was employed to prevent spurious interactions between the repeated slabs. The middle two atomic layers of supercell remained fixed in order to simulate the bulk material and the rest of the atomic layers are allowed to fully relax. Initially, the Fe_3O_4(111) surface had two different terminals: Fe terminal and O terminal. However, after geometry optimization the Fe_3O_4(111) had an obvious surface reconstruction. The Fe terminal exposed to the vacuum layer was covered by the O terminal. Subsequently the twenty-one H_2O molecules were optimized to filled into the vacuum layer based on the density of high temperature water ρ=0.76 g/cm^3.

3. RESULTS AND DISCUSSION

3.1 Adsorption and dissociation processes

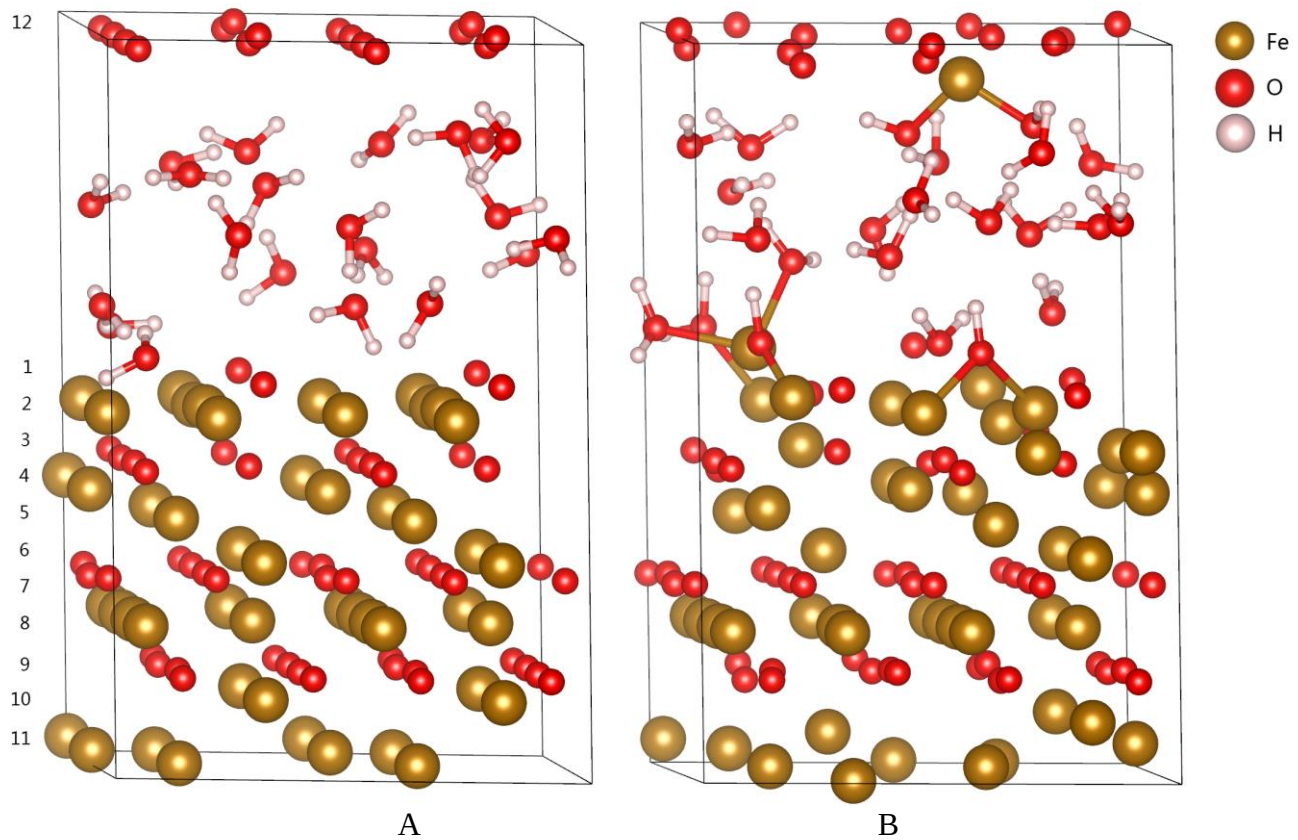

Figure 1. The surface morphologies of Fe_3O_4(111) in 320℃ water (a) in initial state and (b) after 3ps dynamics

Figure 1 shows the surface morphologies of Fe_3O_4(111) in 320℃ high temperature water in initial state and after 3ps dynamics. To clearly denote the calculation results, only the bonding between substrate and solution is labelled. It can be observed in Figure 1b that three H_2O molecules adsorb on

the Fe atoms. The dynamics trajectories of Fe-H_2O bonding are given in Figure 2a. The adsorption time of each H_2O molecule on the surface is different, varying from 440 fs to 1750 fs. After adsorption the H_2O molecules vibrate regularly near the equilibrium position. The average bond lengths of Fe-H_2O are 2.07 Å, 2.09 Å and 2.06 Å respectively, which are close to the DFT calculation result of 2.18 Å [22]. In general, the adsorption of H_2O molecule on the Fe atom is very weak because the absorption energy is only 0.38 eV [22]. Previous studies [23,24] revealed that the H_2O molecule prefers to adsorb on the top site for ferrous metal and its OH group points away from the surface. However, the adsorption of H_2O molecule on the Fe_3O_4(111) surface deviates from the top site of Fe atom, which attributes to the hydrogen bond formation of H atoms of H_2O and O atoms of Fe_3O_4 surface.

It can be found in Figure 1b that the dissociation of some H_2O molecules occurs and the Fe_3O_4(111) surfaces are hydroxylated. The experimental investigations indicated that the outer part of the film consists of a hydroxide film on top of an oxide layer on stainless steels [25]. The spontaneous dissociation processes in the O1, O2, O3 and O4 positions of Figure 1b can be analyzed based on the bonding trajectories of Figure 2b-d. In the O1 position one H_2O molecule first adsorbs on one Fe atom around 580 fs. One O-H bond in this H_2O molecule always vibrates regularly near the equilibrium position as illustrated in the inset of Figure 2b, and its bond length is 0.99 Å, which is in a close agreement with the literature value of 0.97 Å [26]. However, another O-H bond length in this H_2O molecule is increasing after around 1200 fs, which suggests that this O-H bond is broken. The dissociation of H_2O molecule brings about the formation of Fe-OH hydroxide, and its bond length is 1.97 Å, consistent with the literature data of 2.05 Å [27]. Finally this hydroxyl builds another bond with second Fe atom around 1900 fs. In order to analyze the interaction of Fe-OH bonding, the partial density of states (PDOS) is given in Figure 3. The valence electrons of Fe atom are mainly occupied in the 3d orbital, and highly localized near the Fermi level of 2.12 eV. Its electron state passes through the Fermi level. Whereas the valence electrons of O and H atoms are mainly occupied in the 2p and 1s orbitals, respectively. There exist overlapping peaks at the energy level of -19.63 eV, -8.62 eV and -2.97 eV for Fe, O and H atoms in Figure 3a-3d, which suggest that the hybridization bonding between 2p orbital of O atom and 3d orbital of Fe atom occurs. For O and H atoms, it can be observed in Figure 3c and 3d that the electron bands around the fermi level of substrate extend over the solution layer.

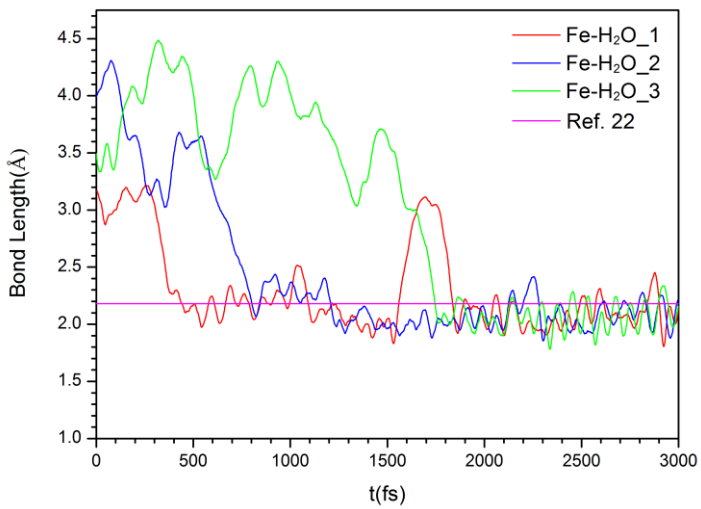

A

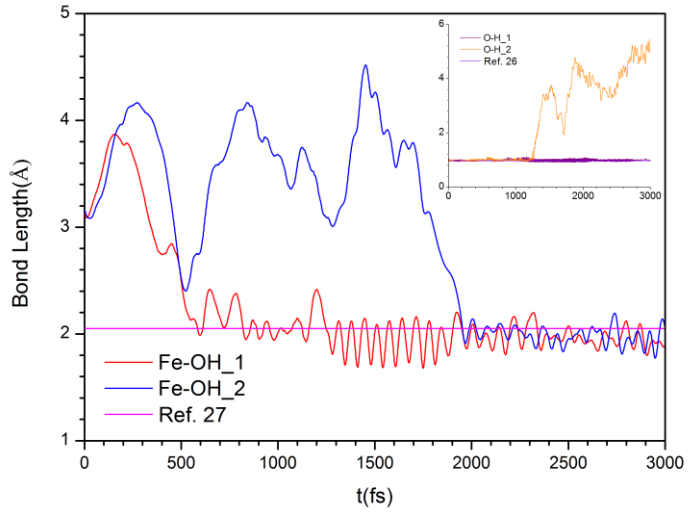

B

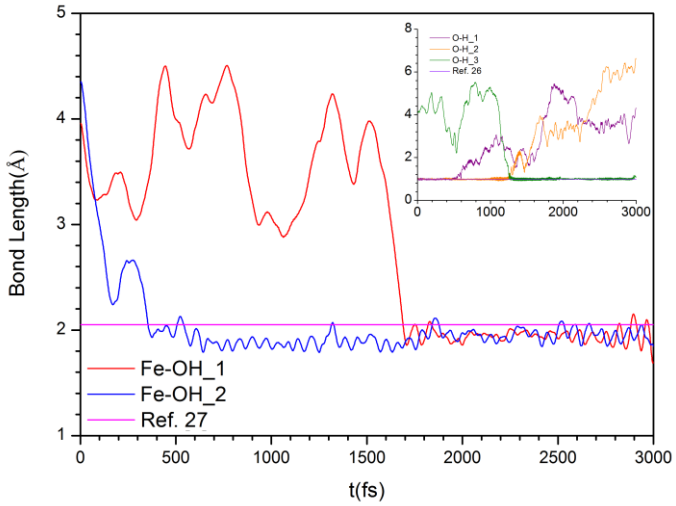

C

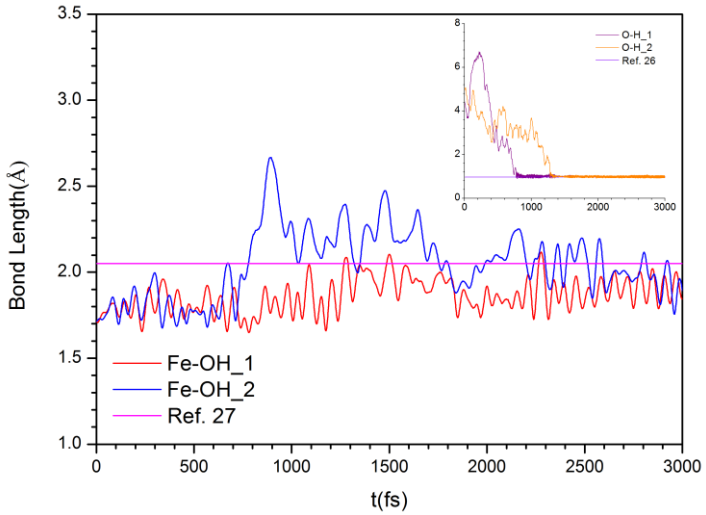

D

Figure 2. The dynamics trajectories for (a) Fe-H_2O bonding in Figure 1b and Fe-OH bonding in the (a) O1, (b) O2, (c) O3 and O4 positions of Figure 1b

The bonding behavior in the O2 position of Figure 1b is similar to that in the O1 position. The H_2O molecule prefers to adsorb on one Fe atom, subsequently the dissociation of this H_2O molecule occurs.

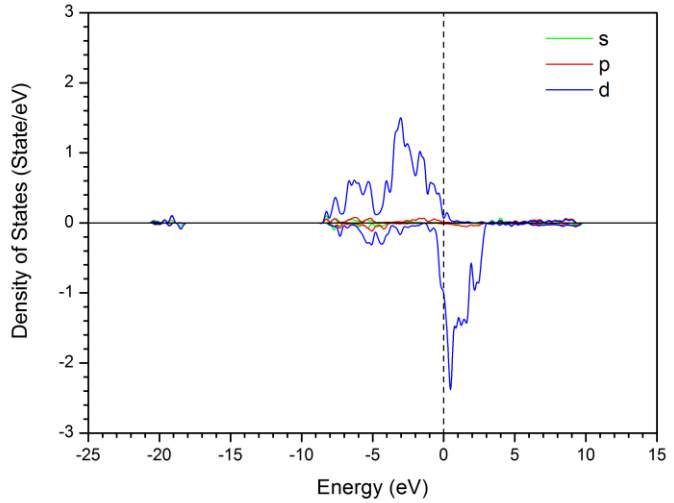

A

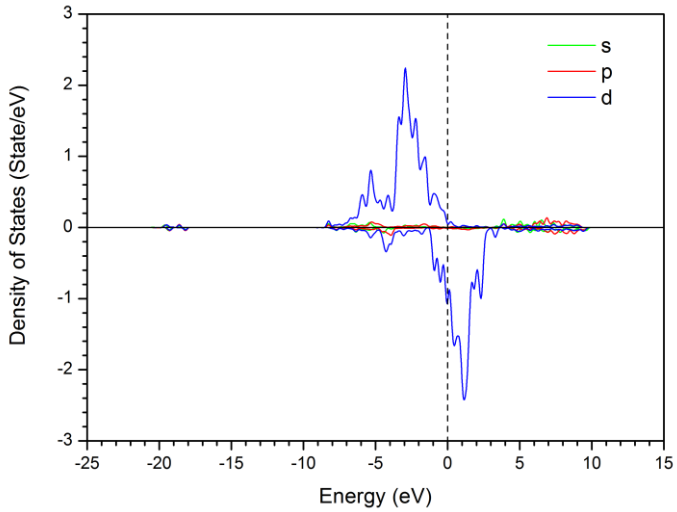

B

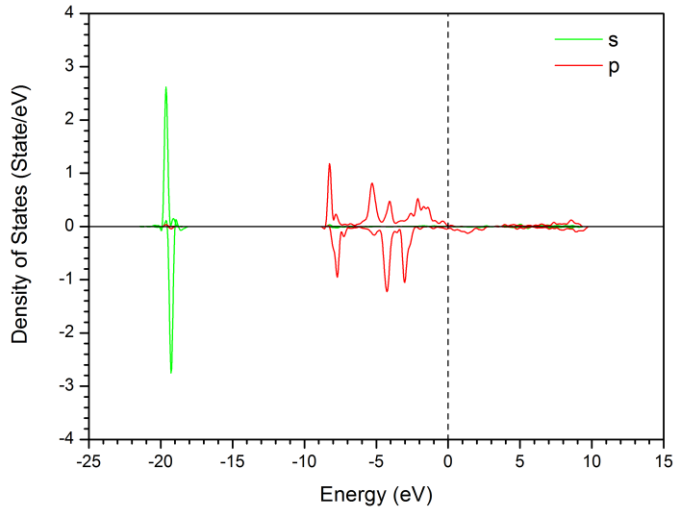

C

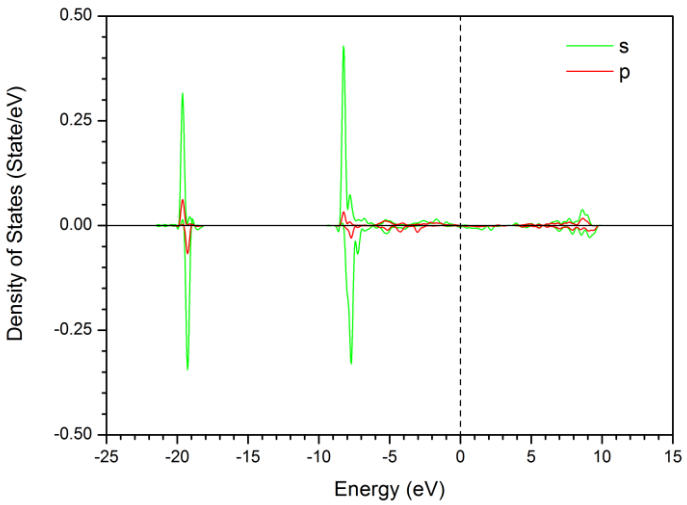

D

Figure 3. The partial density of states (PDOS) for (a) Fe1 atom, (b) Fe2 atom, (c) O atom, (d) H atom in the O2 position of Figure 1b, where Fermi Level=2.12 eV

However, it can be observed in the inset of Figure 2c that the dissociation OH exchanges its proton (O-H_2) with other H_2O molecule (O-H_3), after that the bonding between the hydroxyl and another Fe atom is formed. This bonded Fe atom tends to dissolve in the electrolyte under the joint action of hydroxyl and H_2O molecules, as illustrated in Figure 1b. For the O3 and O4 position of Figure 1b, in fact, these two O atoms belong to the Fe_3O_4 substrate, not H_2O molecules. In the initial stage the Fe-O bonding in the O3 and O4 position has been formed in the substrate, subsequently these two O atoms captures the protons of H_2O molecules to form the hydroxide around 800 fs and 1300 fs, respectively, finally the hydroxide has a tendency to dissolve in the solution.

3.2 Interfacial charge transfer

In order to further understand the reaction behavior on the $Fe_3O_4(111)$ surface, a detailed analysis on the charge transfer is of great importance. The difference charge density of $Fe_3O_4(111)/H_2O$ after 3ps dynamics is shown in Figure 4. The sky blue represents the electron loss, and the yellow represents the electron gain. It can be observed that the charge transfer mainly occurs between the oxide film/ electrolyte interface, whereas the middle layers of substrate and solution only have a little charge transfer. The bader charge analysis is performed to further quantify the charge transfer based on the total density separation with zero flux surfaces. The average electron gain and loss for each kind of atom is shown in Figure 5a. The Fe atoms in the substrate are already in an oxidation state before Fe_3O_4 is immersed in water, which lost about 1.27e on average, whereas the O atoms in the substrate are in a reduction state, which gain about 0.95e on average. After immersion the Fe and O atoms in the substrate continue to lost and gain little electrons respectively, only 0.05e. The O atoms in the aqueous solution gain about 1.16e before immersion, whereas the H atoms lost about 0.58e. These two calculation results are the same with the literature values [28], which suggests that

the calculation reliability is very high. The electron gain of O atoms in the aqueous solution are higher than that of O atoms in the substrate before immersion, and they would relatively gain more electrons after immersion, which is 0.11e on average.

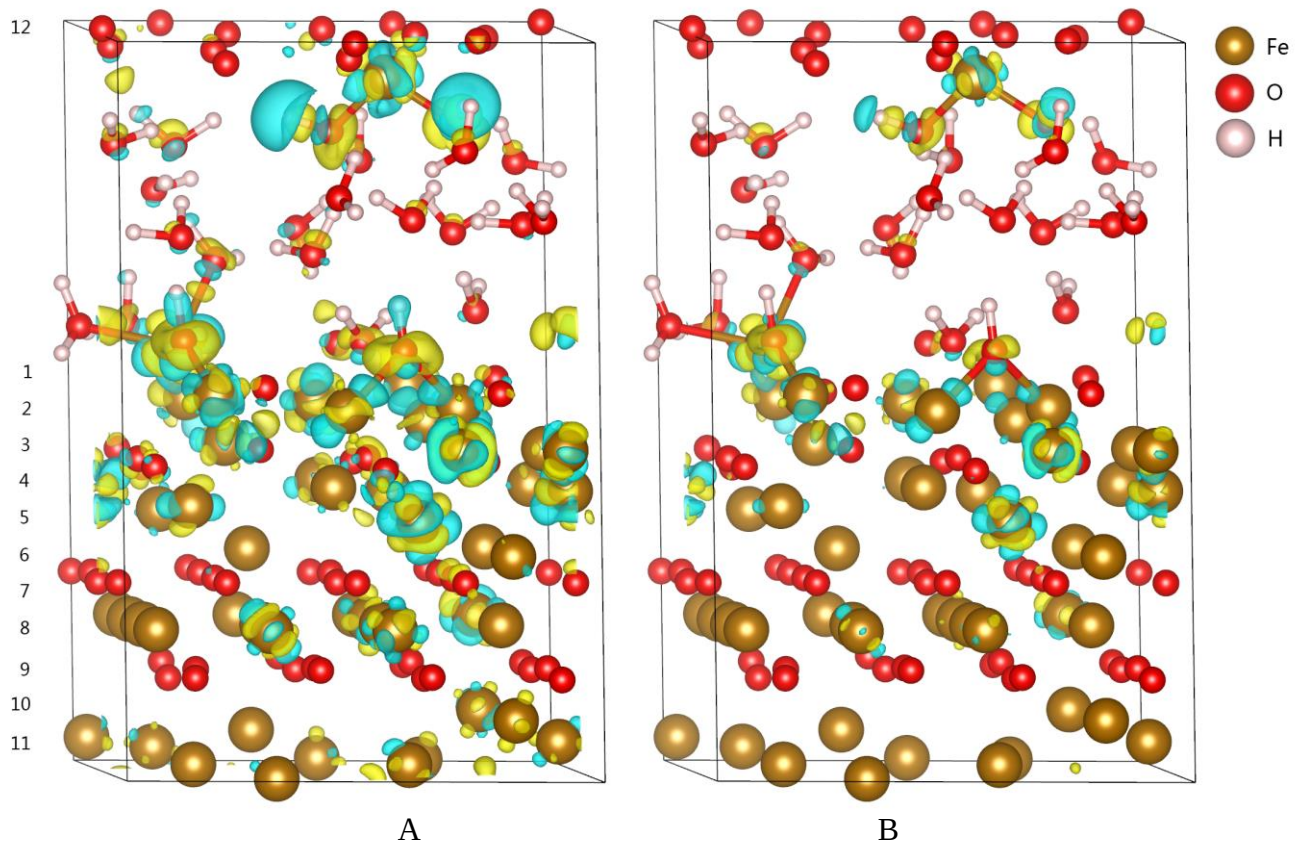

Figure 4. The difference charge density for (a) isosurface level of 0.01 and (b) isosurface level of 0.02 after 3ps dynamics.

Figure 5b gives the average electron gain and loss for each layer of substrate before and after immersion. It can be seen that the layer 2 and layer 12 have an obvious charge transfer. The Fe atoms in the layer 2 lost 0.18e on average after immersion, whereas the O atoms in the layer 12 gain 0.15e on average. Because the charge transfer of inner layers of substrate is not significant, the layer 2 and layer 12 mainly lost and gain electrons from the aqueous solution. The adsorption and dissociation of H_2O molecules on the Fe atoms in the layer 2 gain the electrons of Fe atoms, whereas the O atoms in the layer 12 gains the electrons of H atoms originally belonging to the aqueous solution. However, it is noted that although Figure 5b reveals that the charge of most inner layers nearly has no change after immersion, the atoms inside each layer transfer the electrons each other, as illustrated in Figure 4.

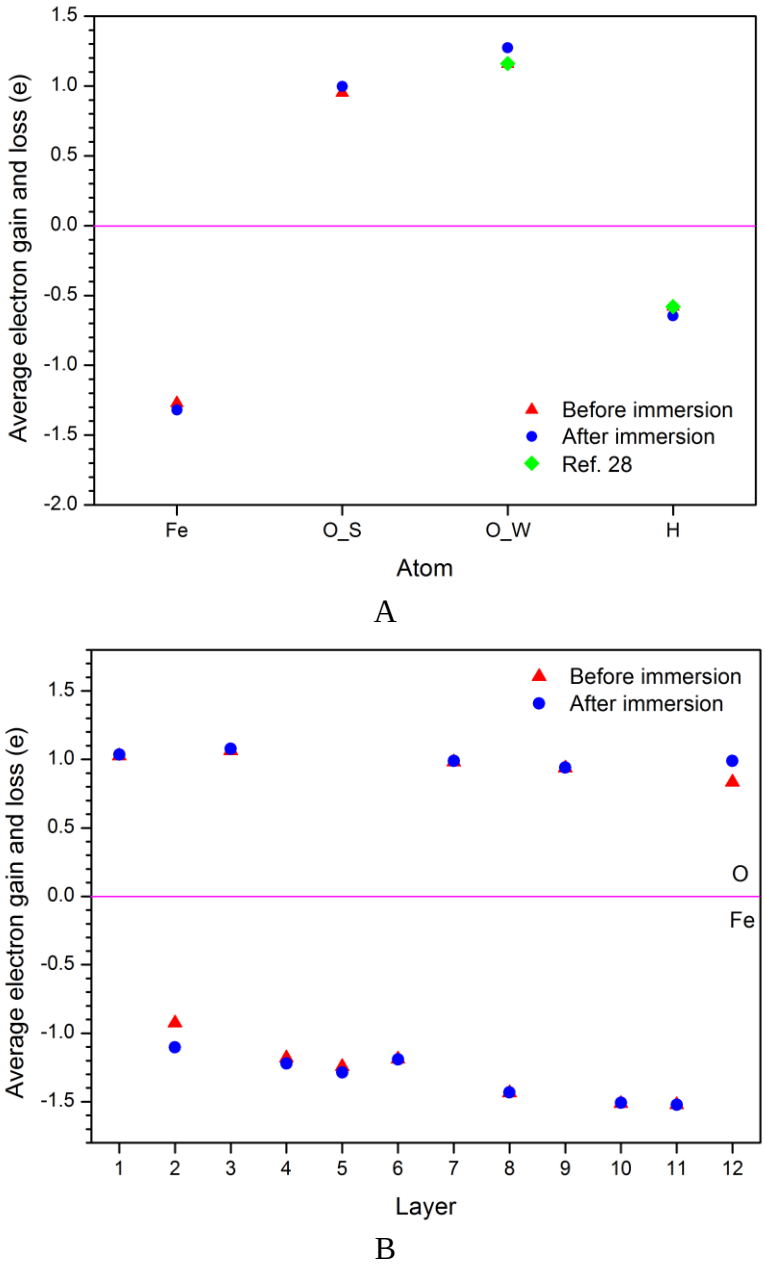

Figure 5. The average electron gain and loss for (a) each kind of atom and (b) each layer of substrate before and after Fe_3O_4 is immersed in water.

4. CONCLUSIONS

A Born-Oppenheimer molecular dynamics simulation within a PAW pseudopotential formalism and the PBE generalized gradient approximation to the exchange-correlation potential was used to clarify the interactions between high temperature water and oxide film Fe_3O_4(111). The model was represented by a twelve-layer Fe_3O_4 slab with a vacuum layer of 10 Å, and the twenty-one H_2O molecules were optimized to filled into the vacuum layer based on the density of high temperature water. After 3ps dynamics calculation, three H_2O molecules adsorb on the Fe atoms and theirs

adsorption sites deviate from the top site of Fe atom because of the hydrogen bond formation of H atoms of H_2O and O atoms of substrate surface. The spontaneous dissociation of some H_2O molecules occurs and the Fe_3O_4(111) surfaces are hydroxylated, in which the proton exchange phenomenon is observed. The partial density of states indicates that the hybridization bonding between 2p orbital of O atom and 3d orbital of Fe atom occurs, and the electron bands around the fermi level of substrate extend over the solution layer. Before the oxide film is immersed in water, the electron gain of O atoms in the aqueous solution are higher than that of O atoms in the substrate, and they would relatively gain more electrons after immersion. The charge transfer mainly occurs between the oxide film/ electrolyte interface, whereas the middle layers of substrate and solution only have a little charge transfer.

ACKNOWLEDGEMENTS
This work was supported by the National Key Research and Development Program of China (Grant No. 2017YFB0702100) and International Science & Technology Cooperation Program of China (Grant No. 2014DFA50800).

References

1. D.X. Chen, E.-H Han and X.Q. Wu, *Corros. Sci.*, 111 (2016) 518
2. X.Y. Zhou, S.N. Lvov, X.J. Wei, L.G. Benning and D.D. Macdonald, *Corros. Sci.*, 44 (2002) 841
3. J.J Chen, Z.P, Lu, Q. Xiao, X.K. Ru, G.D. Han , Z. Chen, B.X. Zhou and T. Shoji, *J. Nucl. Mater.*, 472 (2016) 1
4. S.S. Raiman and G.S. Was, *J. Nucl. Mater.*, 493 (2017) 207
5. S.E. Ziemniak and M. Hanson, *Corros. Sci.*, 44 (2002) 2209
6. Y.L. Han, J.N. Mei, Q.J. Peng, E.-H. Han and W. Ke, *Corros. Sci.*, 112 (2016) 625
7. J. L. Lv, H. Y. Luo and T. X. Liang, *J. Nucl. Mater.*, 466 (2015) 154
8. H. Sun, X.Q. Wu and E.-H. Han, *Corros. Sci.*, 51 (2009) 2840
9. K. Wang, J.H. Wang and W.B. Hu, *Mater. Des.*, 82 (2015) 155
10. G.D. Han, Z.P. Lu, X.K. Ru, J.J. Chen, Q. Xiao and Y.W. Tian, *J. Nucl. Mater.*, 467 (2015) 194
11. W.J. Kuang, E.-H. Han, X.Q. Wu and J.C. Rao, *Corros. Sci.*, 52 (2010) 3654
12. B. Stellwag, *Corros. Sci.*, 40 (1998) 337
13. S. Delaunay, C. Mansour, E.-M. Pavageau, G. Cote, G. Lefevre and M. Fedoroff, *Corrosion*, 67 (2011) 015003
14. W. Andreoni and A. Curioni, *Parallel Comput.*, 26 (2000) 819
15. A. Tilocca and A. Selloni, *J. Phys. Chem. B.*, 108 (2004) 19314
16. N.K. Das, T. Shoji and Y. Takeda, *Corros. Sci.*, 52 (2010) 2349
17. K. Jug, B. Heidberg and T. Bredow, *J. Phys. Chem. C*, 111 (2007) 6846
18. D. Costa, K. Sharkas, M. M. Islam and P. Marcus, *Surf. Sci.*, 603 (2009) 2484
19. G. Kresse and J. Furthmuller, *Phys. Rev. B*, 54 (1996) 11169
20. G. Kresse and D. Joubert, *Phys. Rev. B*, 59 (1999) 1758
21. J.P. Perdew, K. Burke and M. Ernzerhof, *Phys. Rev. Lett.*, 77 (1996) 3865
22. S.L. Liu, X.X. Tian, T. Wang, X.D. Wen, Y.W. Li, J.G. Wang and H.J. Jiao, Phys. *Chem. Chem. Phys.*, 17 (2015) 8811
23. T. Ossowski, J.L.F. Da Silva and A. Kiejn, *Surf. Sci.*, 668 (2018) 144
24. R.R.Q. Freitas, R. Rivelino, F.D.B. Mota, and C.M.C. de Castilho, *J. Phys. Chem. C*, 116 (2012) 20306

25. C.-O.A. Olsson and D. Landolt, *Electrochimica Acta*, 48 (2003) 1093
26. L. Giordano, J. Goniakowski and J. Suzanne, *Phys. Rev. Lett.*, 81 (1998) 1271
27. L. Lopes, J. de Laat and B. Legube, *Inorg. Chem.*, 41 (2002) 2505
28. G. Henkelman, A. Arnaldsson and H. Jonsson, *Comput. Mater. Sci.*, 36 (2006) 354

© 2018 The Authors. Published by ESG (www.electrochemsci.org). This article is an open access article distributed under the terms and conditions of the Creative Commons Attribution license (http://creativecommons.org/licenses/by/4.0/).